



Improving the Slow Release System Using Chitosan-Alginate Nanoparticles with Various Methods for Curcumin

Ageng Trisna Surya Pradana Putra^{1*}, Dwi Siswanta¹ and Adhitasari Suratman¹

¹Department of Chemistry, Faculty of Mathematics and Natural Sciences, Universitas Gadjah Mada, Yogyakarta, 55281, Indonesia.

Authors' contributions

This work was carried out in collaboration between all authors. All authors read and approved the final manuscript.

Article Information

DOI: 10.9734/ACSJ/2016/25989

Editor(s):

(1) Georgiy B. Shul'pin, Semenov Institute of Chemical Physics, Russian Academy of Sciences, Moscow, Russia.

Reviewers:

- (1) Anonymous, Delaware State University, USA.
(2) Dina M. Abd-Alaziz, National organization for Drug Control and Research (NODCAR), Egypt.
(3) Anonymous, Khon Kaen University, Thailand.
(4) Yongqiang Wen, University of Science and Technology Beijing, China.

Complete Peer review History: <http://sciencedomain.org/review-history/14746>

Original Research Article

Received 29th March 2016
Accepted 10th May 2016
Published 23rd May 2016

ABSTRACT

Biodegradable polymeric materials have been used as a drug delivery system due to its encapsulation, release system and less toxic properties. Chitosan-alginate nanoparticles were prepared by ionotropic pre-gelation of alginate core, followed by polyelectrolyte complexation of chitosan and curcumin was chosen as a model drug.

Aims: The aim of this study was to evaluate the possibility of chitosan-alginate nanoparticles as carriers for curcumin using various methods.

Methodology: This preparation was divided into 4 methods to produce Alginate-Calcium-Chitosan (ACaK), Alginate-Chitosan-Calcium (AKCa), Chitosan-Alginate-Calcium (KACa) and Alginate-Chitosan (AK) nanoparticles. The amount of drug entrapped was determined by shaking the solution and then supernatant was analyzed for drug loading by measuring the absorbance, morphology, particle sizes and kinetics.

Results: The encapsulation efficiency was up to 85% in higher drug-polymer ratio and the effect of egg-box model made diameter of nanoparticles between 51 and 90 nm. The kinetic model of

*Corresponding author: E-mail: ageng.trisna69@yahoo.com;

desorption for Alginate-Calcium-Chitosan, Alginate-Chitosan-Calcium and Chitosan-Alginate-Calcium nanoparticles followed Korsmeyer-Peppas.

Conclusion: This study suggests that these materials serve as suitable for uptake in capillary due to their nano-sized range and could stay long time into bloodstream.

Keywords: Curcumin; release system; drug delivery; nanoparticles; kinetic.

1. INTRODUCTION

Curcumin or (Diferuloylmethane) is a polyphenol derived from the herb *Curcuma longa* and commonly known as turmeric [1] (Fig. 1). Curcumin has anti-carcinogenic [2-5], anti-HIV [6], anti-inflammatory [7-12], antioxidant [13-15] and antitumor properties [16]. Despite extensive research and development, the properties of curcumin in aqueous solution were low bioavailability and poor solubility [17]. Therefore, curcumin is often limited by its potential to reach the site of therapeutic action. Curcumin has been reported that it is complex with cyclodextrin [18] and phospholipids [19] or encapsulated in solid lipid microparticles such as chitosan [20] and albumin [21]. A drug delivery system has opened up new possibilities in targeted and sustained release of drugs by nanotechnology [22]. A drug delivery system was designed by tiny nanoparticles and it can reach less accessible sites in the body. Controlled release of the drug from the nanoformulations could maintain steadier levels of drug in bloodstream for longer durations. Sustained release of drug can be achieved by encapsulation the active ingredient in a polymer matrix.

Chitosan (K) and sodium alginate (A) are extensively used in encapsulation of drug for the purpose of the sustained release [23]. Sodium alginate is an anionic polysaccharide obtained from marine algae and it is a water-soluble natural copolymer composed of guluronic and

mannuronic acid units. In addition, chitosan is deacetylate derivatives of chitin, composed by β -(1, 4)-2-amino-2-deoxy-D-glucopyranose units and small amount of N-acetyl-D-glucosamine residues [24]. These are polysaccharide polymers, formed from repeating units (either mono- or di- saccharides) joined together by glycosidic bond [25]. They have many properties of an ideal carrier for drug delivery such as biocompatibility, biodegradability, low cost and non-toxicity [26]. Encapsulation of hydrophobic drugs into an aqueous nanoparticulate system has been attempted so as to deliver such drugs with their full potential [27]. Rajaonarivony et al. [28] reported that poly-L-lysine/alginate nanoparticles were produced using a pre-gel method.

The objective of this study was to evaluate the possibility of chitosan-alginate nanoparticles as carriers for curcumin. The challenge was to entrap hydrophobic molecules such as curcumin into hydrophilic nanoparticles formed by ionotropic pre-gelation of the alginate core followed by chitosan polyelectrolyte complexation. The final samples were characterized using Fourier Transform Infrared spectrometer (FTIR), Scanning Electron Microscope (SEM) and Transmission Electron Microscope (TEM), respectively. In addition, curcumin release was analyzed using Ultraviolet-Visible (UV-Vis). The release properties of nanoparticles in ratio of phosphate buffered saline and ethanol (80:20) at pH 7.4 were also studied.

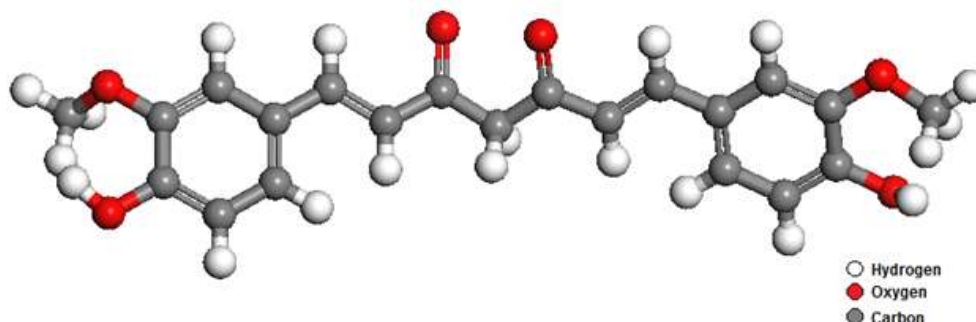


Fig. 1. Chemical structure of curcumin

2. MATERIALS AND METHODS

2.1 Preparation of Curcumin Loaded Chitosan-Alginate Nanoparticles

Sodium alginate (400 cps) and calcium chloride solutions were prepared by dissolving the chemicals in distilled water. However, chitosan (DD 93.8%) was dissolved in 1% acetic acid solution and curcumin (CC ≥94%) was dissolved in ethanol (97%). The pH of the sodium alginate and chitosan solution was adjusted to 5 using hydrochloric acid and sodium hydroxide, respectively. All chemicals were used without further purification.

This preparation was divided into 4 methods to produce Alginate-Calcium-Chitosan (ACaK), Alginate-Chitosan-Calcium (AKCa), Chitosan-Alginate-Calcium (KACa) and Alginate-Chitosan (AK) nanoparticles. Calcium chloride solution 0.07% (w/v) (2.5 mL) was added dropwise to 25 mL aqueous sodium alginate 0.12% (w/v) while stirring magnetically 2000 rpm for 30 minutes and kept at room temperature. Two mL of curcumin solution 1% (w/v) and 10 mL chitosan solution 0.05% (w/v) were added into the resultant calcium alginate pre-gel, stirred magnetically 1500 rpm for an hour, and kept at room temperature called as ACaK. AKCa were obtained as ACaK, but calcium chloride solution was added after mixing alginate and chitosan solution. KACa were obtained as AKCa, but 10 mL alginate solution was added into 25 mL of chitosan solution. On the other hand, chitosan solution (10 mL) and 23 mL distilled water were added into 25 mL alginate solution without calcium, stirred magnetically 1500 rpm for an hour, and kept at room temperature called as AK.

All of the resultant suspensions as ACaK, AKCa, KACa and AK were equilibrated overnight at room temperature to allow nanoparticles. Each result was separated by centrifugation at 4°C to form uniform particle sizes. Particles were dried using a freeze dryer overnight. Blank nanoparticles were obtained as a previous procedure of curcumin loaded nanoparticles, but they were not added by curcumin solution. They were called as AK-0, ACaK-0, AKCa-0 and KACa-0.

The amount of drug entrapped was determined as shown in the following equation by centrifugation of the dispersion and then supernatant was analyzed for drug loading by

measuring the absorbance at 426 nm in UV spectrophotometer. The confirmation of drug loading was done by comparing optical absorbance of nanoformulations with and without drug loading.

$$\% \text{ encapsulation} = (\text{drug input (mg)} - \text{drug in supernatant (mg)}) / (\text{drug input (mg)}) \times 100\%$$

The morphology, measurements of particle sizes and functional groups of the nanoparticles were performed using Scanning Electron Microscope (SEM) (JEOL, JSM-6510), Transmission Electron Microscope (TEM) (JEOL, JEM-1400) and Fourier Transform Infrared spectra (FTIR), respectively. Sample preparation using FTIR was taken with KBr pellets on a FTIR spectrometer (Shimadzu-Prestige 21).

2.2 *In vitro* Release of Curcumin

To establish curcumin release profiles from nanoparticles, curcumin loaded nanoparticles were separated from matrix by shaking at 37°C in various times. At appropriate intervals, five mL solution was taken and analyzed using UV spectrophotometer. Each sample pretreatment for SEM and TEM was used to dry treatment. The mathematical models such as zero-order, first-order, Higuchi, and Korsmeyer-Peppas equations were fitted to individual dissolution data.

Zero-order model is used to describe drug dissolution from pharmaceutical dosage forms that do not aggregate and release the drug slowly. It can be represented by the equation: $Q_0 - Q_t = K_0 \cdot t$, where K_0 is the zero order release constant expressed in units of concentration/time, Q_0 is the initial amount of drug in the solution and Q_t is the amount of drug dissolved in time t . Data obtained from *in vitro* drug release studies were plotted as cumulative amount of drug release vs time [29].

First order model has also been used to describe absorption and/or elimination of some typical drugs. This release model can be expressed by the equation: $dC/dt = -K \cdot C$, where K is the first order rate constant expressed in units of time^{-1} , t is the time and C is concentration of drug. The data obtained were plotted as log cumulative percentage of drug remaining vs time which would yield a straight line with a slope of $(-K) / 2.303$ [30].

Higuchi model describes drug release from a matrix system and based on hypotheses that (i) initial drug concentration in the matrix is much higher than drug solubility; (ii) drug diffusion takes place only in one dimension (edge effect must be negligible); (iii) drug particles are much smaller than system thickness; (iv) matrix swelling and dissolution are negligible; (v) drug diffusivity is constant; and (vi) perfect sink conditions are always attained in the release environment. The expression of this model is given by the equation: $f_t = Q = A \sqrt{(D(2C - C_s) C_s \cdot t)}$, where C is the drug initial concentration, C_s is the drug solubility in the matrix media, D is the diffusion coefficient in the matrix substance, f_t or Q is the amount of drug released in time (t) per unit area (A) and t is time. In addition, the model is possible to simplify the Higuchi model as $f_t = Q = K_H \cdot t^{1/2}$ [31], where K_H is the Higuchi dissolution constant [32]. The data obtained were plotted as cumulative percentage drug release vs square root of time [33].

Korsmeyer-Peppas model has been used to describe drug release from a polymeric system equation. This equation can be expressed as $M_t / M_\infty = k \cdot t^n$, where k is the release rate constant, M_t / M_∞ is a fraction of drug released at time (t) and n is the release exponent. The n value is used to characterize different release for cylindrical shaped matrices [34]. In this case of cylindrical tablet, $0.45 \leq n$ corresponds to a Fickian diffusion mechanism, $0.45 < n < 0.89$ to non-Fickian transport, $n = 0.89$ to case II transport (relaxation), and $n > 0.89$ to super case II transport [35]. To study the release kinetics, data obtained from *in vitro* drug release studies were plotted as log cumulative percentage drug release vs log time. To find out the mechanism of drug release, the first 60% drug release data should be used.

3. RESULTS AND DISCUSSION

3.1 Preparation of Chitosan-Alginate Nanoparticles

Chitosan-alginate nanoparticles were obtained spontaneously under very mild conditions. Preparation of chitosan-alginate nanoparticles appeared some typical peaks. IR spectra of chitosan (Fig. 2 (a)) showed the broad band at 3448 cm^{-1} corresponded to the amine and hydroxyl groups. The absorption bands of carbonyl stretching of the secondary amide (amide I band) and the bending vibrations of the N-H (amide II band) were at 1651 cm^{-1} and 1597

cm^{-1} , respectively. The peak of secondary hydroxyl group was observed at 1087 cm^{-1} . The band in the IR spectra of sodium alginate (Fig. 2 (b)) at 1419 cm^{-1} and 1612 cm^{-1} was assigned to symmetric and asymmetric stretching peaks of carboxylate salt groups. In addition, the absorption band of alginate at 1612 cm^{-1} shifted to 1627 cm^{-1} after reacting with chitosan (Fig. 2 (c)) as polyelectrolyte complexation. The AK-0 was used to control between other samples added by calcium ions (Ca). FTIR spectra of sodium alginate and calcium ions appeared a specific peak at 1080 cm^{-1} indicating hydroxyl groups interacted with calcium ions. The peaks of ACaK-0 and KACa-0 were observed at 1620 cm^{-1} and 1604 cm^{-1} , respectively (Fig. 2 (d and e)). They indicate that calcium ions interacted with carboxylate ions of sodium alginate to form an egg-box model. The IR spectra of AKCa-0 (not shown) had identical peaks with ACaK-0.

The FTIR was adopted to characterize the potential interaction between 2 polymers and calcium ions into nanoparticles. As shown in Fig. 3 (a), IR spectra of curcumin had specific peaks at 1427 cm^{-1} and 1512 cm^{-1} as aromatic rings, Carbon double bond was at 1627 cm^{-1} , methoxy stretching peak appeared at 2854 cm^{-1} and a broad band at 3510 cm^{-1} was attributed to the stretching vibration of the OH groups. IR spectra of AK that observed the asymmetrical stretching of carboxyl groups at 1627 cm^{-1} shifted to 1635 cm^{-1} (Fig. 3 (b and c)), which probably indicates that curcumin molecule was filled in the polymeric network. In addition, these results indicate that carboxylate groups of alginate associate with ammonium groups of chitosan through electrostatic interactions to form the polyelectrolyte complexation. The IR spectra of ACaK-0 and ACaK at 1620 cm^{-1} shifted to 1627 cm^{-1} and 3425 cm^{-1} to 3433 cm^{-1} (Fig. 3 (d and e)). In addition, IR spectra of KACa-0 and KACa at 1604 cm^{-1} shifted to 1627 cm^{-1} and 3441 cm^{-1} shifted to 3433 cm^{-1} (Fig. 3 (f and g)).

An analysis of electron microscopy was confirmed the presence of nanoparticles and provided morphological information of the typical curcumin loaded chitosan-alginate nanoparticles using the transmission electron microscope (TEM) and scanning electron microscope (SEM), respectively. Fig. 4 showed the comparison of 2 methods between ACaK and AKCa because calcium ion had unique characteristics to design small particles (Fig. 5). Particle sizes were about between 51 and 90 nm depending on methods and particles were seen to be spherical solid.

The interaction between alginate and calcium ions produced egg-box model and the diameters were smaller than without producing egg-box

model because calcium-alginate complex in pre-gel state was enveloped by chitosan as cationic polymer (Fig. 6).

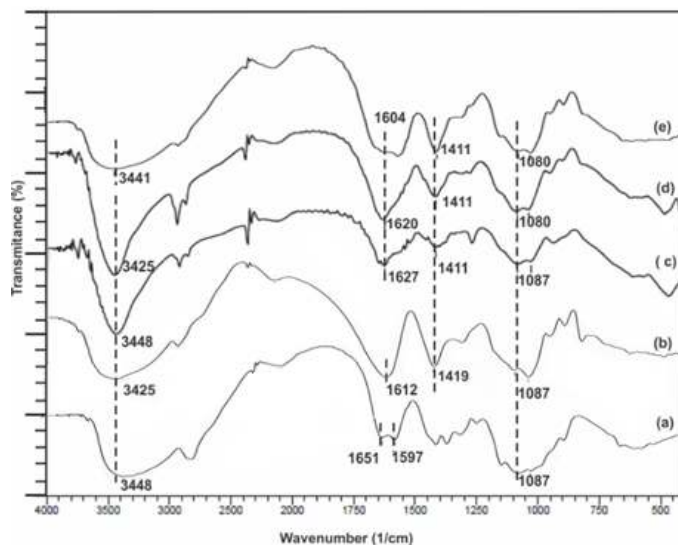


Fig. 2. FTIR spectra of chitosan (a), sodium alginate (b), AK-0 (c), ACaK-0 (d) and KACa-0 (e)

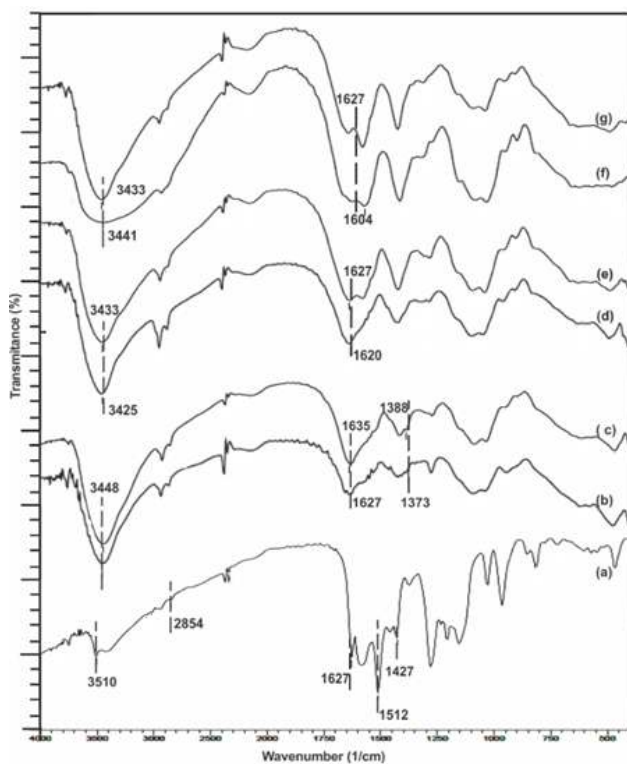


Fig. 3. FTIR spectra of curcumin (a), AK-0 (b), AK (c), ACaK-0 (d), ACaK (e), KACa-0 (f) and KACa (g)

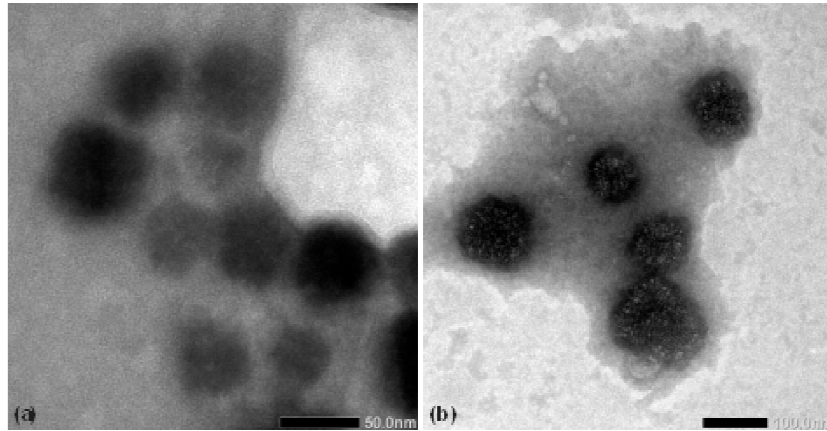


Fig. 4. TEM Images of curcumin loaded nanoparticles, ACaK (a), AKCa (b)

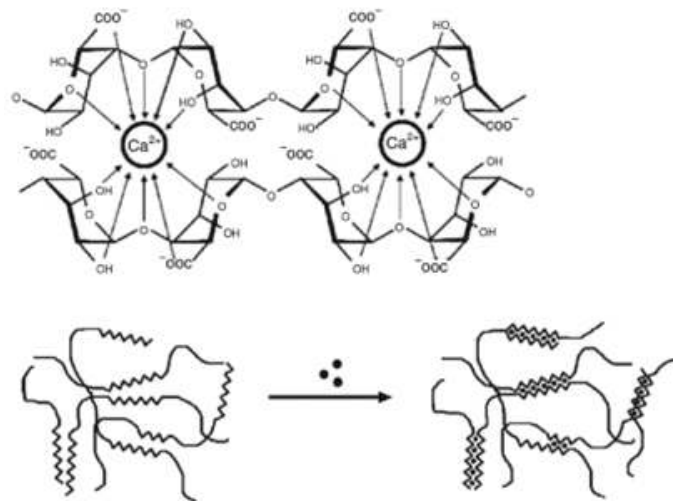


Fig. 5. Alginate-egg-box model. Chelate of cationic divalent (above), forming the junction between the chain (bottom) ($\text{Ca}^{2+} = \bullet$)

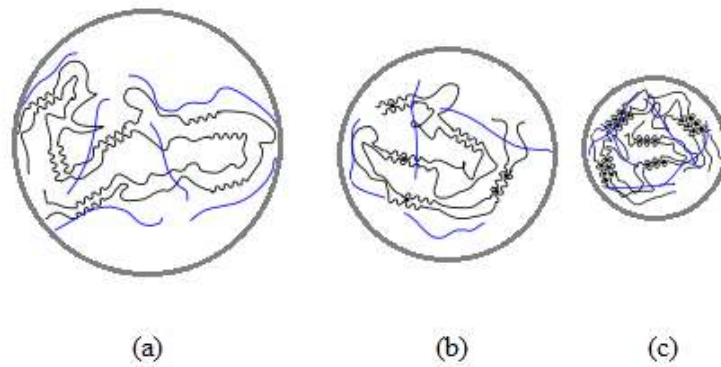


Fig. 6. Illustration of ACaK nanoparticles, alginate (black), chitosan (blue), Ca^{2+} (dot), without Ca^{2+} (a), with Ca^{2+} 0.6 (b) and 0.9 mM (c)

Fig. 7 showed appearances in the form of dry solids between with and without calcium ions. If they were dispersed, they would be able to decompose easily into nanometer sizes. Encapsulation efficiencies of ACaK, AKCa and KACa were 85.38, 65.00 and 73.22%, respectively (Fig. 8). The result shows calcium ions interacted between alginate and chitosan because the matrix produced egg-box model and nano-sized particles. Therefore, these nanoparticles are effective to entrap curcumin as a drug model. The interaction between Ca^{2+} and alginate could be the best method to design particle sizes to compare other nanoparticle methods and also these treatments were easily methods to large production.

3.2 *In vitro* Release of Curcumin

The release of ACaK has been reached the slowest because ACaK produced egg-box models that have an ability to control curcumin release from matrix slowly, but AKCa has the fastest curcumin release because they could not produce egg-box models well and the effect is that only little curcumin entrapped into matrix between alginate and chitosan. In many experimental situations, including the case of drug release from swellable polymeric systems, the mechanism of drug release diffusion deviates from the Fickian equation and follows a non-Fickian behavior (anomalous). In the cases, the following general equation or its logarithmic form

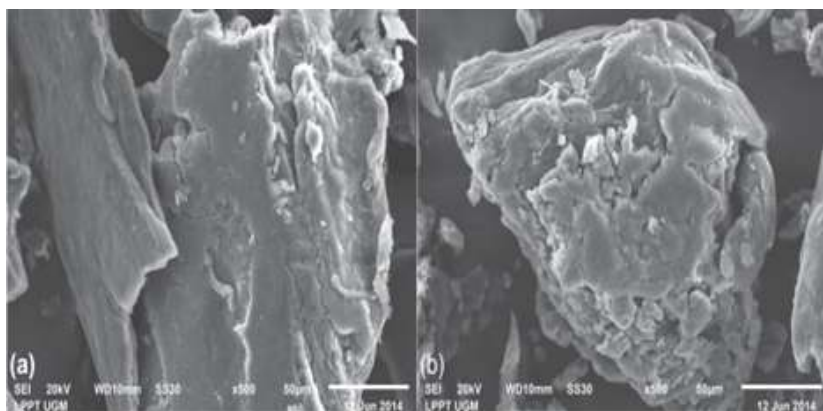


Fig. 7. SEM Images of nanoparticles without (a) and with calcium ions (b)

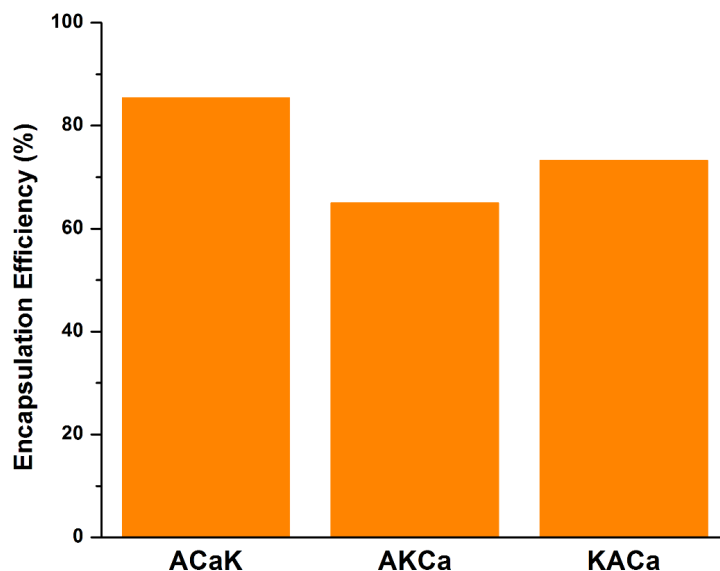


Fig. 8. Encapsulation efficiency of ACaK, AKCa and KACa nanoparticles

can be used as cylindrical tablets, values of n between 0.45 and 0.89 indicate both diffusion and swelling controlled drug release (anomalous transport). Values above 0.89 indicate case-II transport which is related to polymer relaxation during hydrogel swelling and values below 0.45 indicate that drug release from polymer is due to Fickian diffusion.

The n and k values were obtained from releasing curves (Fig. 9) and presented in Table 1. The n value is the diffusional exponent that can be related to the drug transport mechanism. The ACaK, AKCa and KACa fitted to Korsmeyer-Peppas' model. The values of n for ACaK, AKCa and KACa were 0.591, 0.333 and 0.283, respectively. The ACaK mechanism followed diffusion and erosion, but both AKCa and KACa

mechanisms only followed diffusion. Therefore, ACaK was very effective to be a drug release system because a drug model could be released slower than others and then the matrix will be broken by erosion after releasing curcumin slowly. In addition, the ACaK produced egg-box models easily because calcium ions were interacted into carboxylic groups of alginate well, but the first interactions between alginate and chitosan of AKCa and KACa did not produce egg-box models because carboxylate groups of alginate had interacted with amine of chitosan to form polyelectrolyte complex. Therefore, calcium ions did not have ability to interact into functional group of alginate and ethanol was added into phosphate buffered saline to increase the solubility of curcumin, then the kinetic model could be reached gap clearly than others.

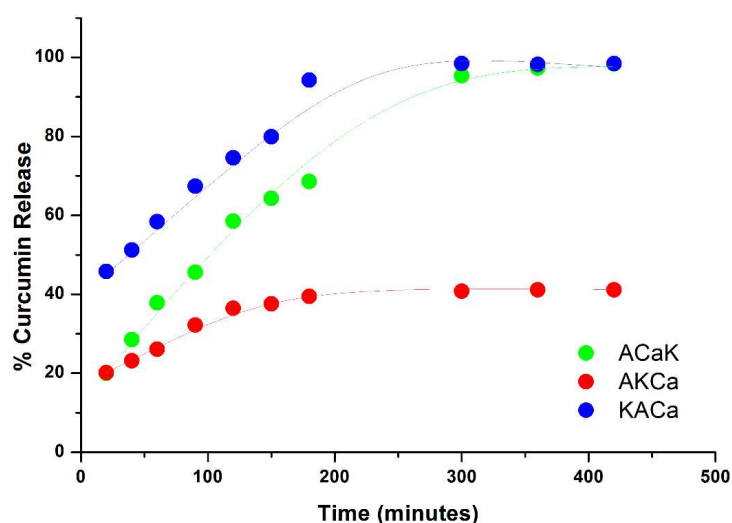


Fig. 9. *In vitro* curcumin release (%) from ACaK, AKCa and KACa in mixing PBS and ethanol solution at 37°C

Table 1. Estimated parameters and drug release mechanisms of curcumin loaded chitosan-alginate nanoparticles

Nanoparticle	Kinetic model	Kinetic constant (k)	r^2	Diffusional exponent (n)
ACaK	Zero order	0.198	0.928	
	First order	0.010	0.976	
	Higuchi	5.266	0.984	
	Korsmeyer-Peppas	3.327	0.995	0.591
AKCa	Zero order	0.048	0.698	
	First order	0.001	0.722	
	Higuchi	1.341	0.838	
	Korsmeyer-Peppas	7.091	0.968	0.333
KACa	Zero order	0.133	0.818	
	First order	0.013	0.937	
	Higuchi	3.606	0.918	
	Korsmeyer-Peppas	19.191	0.977	0.283

4. CONCLUSION

In this study, the possibility to entrap hydrophobic curcumin was successfully compounded within chitosan-alginate nanoparticles using a very simple ionotropic pre-gelation and polyelectrolyte complex techniques. The diameters of nanoparticles were obtained between 51 and 90 nm. The encapsulation efficiency was up to 85% in higher drug-polymer ratio. The kinetic model of desorption for ACaK, AKCa and KACa nanoparticles followed Korsmeyer-Peppas. These materials are suitable for uptake in capillary due to their nano-sized range and could stay long time into bloodstream.

ACKNOWLEDGEMENTS

We are grateful to TANOTO FOUNDATION with grant number 224/TF-JKT/IV/2014, for financial support of this work.

COMPETING INTERESTS

All authors had financial support from TANOTO FOUNDATION for the submitted work; no financial relationships with any organizations that might have an interest in the submitted work in the previous three years; no other relationships or activities that could appear to have influenced the submitted work.

REFERENCES

1. Anderson AM, Mitchell MS, Mohan RS. Isolation of curcumin from turmeric. *J. Chem. Educ.* 2000;77:359–360.
2. Aggarwal BB, Kumar A, Bharti AC. Anticancer potential of curcumin: Preclinical and clinical studies. *Anticancer Res.* 2003;23:363-398.
3. Rao CV, Rivenson A, Simi B, Reddy BS. Chemoprevention of colon carcinogenesis by dietary curcumin, a naturally occurring plant phenolic compound. *Cancer Res.* 1995;55:259-266.
4. De R, Kundu P, Swarnakar S, Ramamurthy T, Chowdhury A, Nair GB, Mukhopadhyay AK. Antimicrobial activity of curcumin against helicobacter pylori isolates from India and during infections in mice. *Antimicrob. Agents Chemother.* 2009;53:1592–1597.
5. Wang Y, Lu Z, Wu H, Lv F. Study on the antibiotic activity of microcapsule curcumin against foodborne pathogens. *Int. J. Food Microbiol.* 2009;136:71–74.
6. Jordan WC, Drew CR. Curcumin: A natural herb with anti-HIV activity. *J. Natl. Med. Assoc.* 1996;88:333–334.
7. Lantz RC, Chen GJ, Solyom AM, Jolad SD, Timmermann BN. The effect of turmeric extracts on inflammatory mediator production. *Phytomedicine.* 2005;12:445-452.
8. Ammon HP, Wahl MA. Pharmacology of curcuma longa. *Planta Med.* 1991;57:1-7.
9. Brouet I, Ohshima H. Curcumin, an anti-tumor promoter and anti-inflammatory agent, inhibits induction of nitric oxide synthase in activated macrophages. *Biochem. Biophys. Res. Commun.* 1995;206:533-540.
10. Dikhsit M, Rastogi L, Shukla R, Srimal RC. Prevention of ischaemia-induced biochemical changes by curcumin and quinidine in the cat heart. *Ind. J. Med. Res.* 1995;101:31-50.
11. Srimal RC, Dhawan BN. Pharmacology of diferyloyl methane (curcumin), a non-steroidal anti-inflammatory agent. *J. Pharm. Pharmacol.* 1973;25:447–452.
12. Aggarwal BB, Harikumar KB. Potential therapeutic effects of curcumin: The anti-inflammatory agent against neurodegenerative cardiovascular, pulmonary, metabolic, autoimmune and neoplastic diseases. *Int. J. Biochem. Cell Biol.* 2009;41:40–59.
13. Ruby AJ, Kuttan G, Babu KD, Rajasekharan KN, Kuttan R. Antitumor and antioxidant activity of natural curcuminoids. *Cancer Lett.* 1995;94:79-83.
14. Pizzo P, Scapin C, Vitadello M, Florean C, Gorza, L. Grp 94 acts as a mediator of curcumin-induced antioxidant defence in myogenic cells. *J. Cell. Mol. Med.* 2010;14:970–981.
15. Sugiyama Y, Kawakishi S, Osawa T. Involvement of the diketone moiety in the antioxidative mechanism of tetrahydrocurcumin. *Biochem. Pharmacol.* 1996;52:519–525.
16. Lee YK, Lee WS, Hwang JT, Kwon DY, Surh YJ, Park OJ. Curcumin exerts anti-differentiation effect through AMPKR-PPARin 3T3-L1 adipocytes and anti-proliferatory effect through AMPKR/COX-2 in cancer cells. *J. Agric. Food Chem.* 2009;57:305–310.
17. Anand P, Kunnumakkara AB, Newman RA, Aggarwal BB. Bioavailability of curcumin: Problems and promises. *Mol. Pharm.* 2007;4:807-818.

18. Yallapu MM, Jaggi M, Chauhan SC. Poly (β -cyclodextrin)/curcumin self-assembly: A novel approach to improve curcumin delivery and its therapeutic efficacy in prostate cancer cells. *Macromol. Biosci.* 2010;10:1141–1151.
19. Maiti K, Mukherjee K, Gantait A, Saha BP, Mukherjee PK. Curcumin-phospholipid complex: Preparation, therapeutic evaluation and pharmacokinetic study in rats. *Int. J. Pharm.* 2007;330:155–163.
20. Das RK, Kasoju N, Bora U. Encapsulation of curcumin in alginate-chitosan-pluronic composite nanoparticles for delivery to cancer cells. *Nanomedicine.* 2010;6:153–160.
21. Gupta V, Aseh A, Rios CN, Aggarwal BB, Mathur AB. Fabrication and characterization of silk fibroin-derived curcumin nanoparticles for cancer therapy. *Int. J. Nanomed.* 2009;4:115–122.
22. Dinauer N, Balthasar S, Weber C, Kreuter J, Langer K, Brisen HV. Selective targeting of antibody-conjugated nanoparticles to leukemic cells and primary T-lymphocytes. *Biomaterials.* 2005;26:5898-5900.
23. Chopra M, Kaur P, Bernela M, Thakur R. Synthesis and optimization of streptomycin loaded chitosan-alginate nanoparticles. *Int. J. Sci. Tech Res.* 2012;1:31-34.
24. Martins AF, Bueno PVA, Almeida EAMS, Rodrigues FHA, Rubira AF, Muniz EC. Characterization of N-trimethyl chitosan/alginate complexes and curcumin release. *Int. J. Biol. Macromol.* 2013;57:174-184.
25. Varki A, Freeze EJ, Stanley P, Bertozzi C, Hart G, Etzler M. *Essentials of glycobiology.* Cold Spring Harb Lab. Press. 2008;62:770-779.
26. Angshuman B, Bhattacharjee SK, Mahanta R, Biswanth M, Bandyopadhaya SK. Alginate based nanoparticulate drug delivery for anti HIV drug lopinavir. *JGPT.* 2010;2:126-132.
27. Li P, Dai NY, Zhang PJ, Wang QA, Wei Q. Chitosan-alginate nanoparticles as a novel drug delivery system for nifedipine. *Int. J. Biomed. Sci.* 2008;4:221-228.
28. Rajaonarivony M, Vauthier C, Coiarraze G, Puisieux F, Couvreur P. Development of a new drug carrier made from alginate. *J. Pharm. Sci.* 1993;82:912-917.
29. Narasimhan B, Mallapragada SK, Peppas NA. *Encyclopedia of controlled drug delivery: Release kinetics, data interpretation.* John Wiley and Sons, Inc: New York. 1999;921.
30. Hadjiioannou TP, Christian GD, Koupparis MA. *Quantitative calculations in pharmaceutical practice and research.* VCH Publishers: Inc, New York; 1993.
31. Higuchi T, Mechanism of sustained action medication, theoretical analysis of rate of release of solid drugs dispersed in solid matrices. *J. Pharm. Sci.* 1963;52(12):1145-1149.
32. Arhewoh MI, Okhamafe OA. An overview of site-specific delivery of orally administered protein/ peptides and modelling considerations. *J. Med, Biomed. Res.* 2004;3:7-20.
33. Silvina AB, Maria CL, Claudio JS. *In-vitro* studies of diclofenac sodium controlled-release from biopolymeric hydrophilic matrices. *J. Pharm. Pharm. Sci.* 2002;5:213-219.
34. Ritger PL, Peppas NA. A simple equation for description of solute release II Fickian and anomalous release from swellable devices. *J. Control. Rel.* 1987;5:37-42.
35. Siepmann J, Peppas NA. Modeling of drug release from delivery systems based on hydroxypropyl methylcellulose (HPMC). *Adv. Drug Deliv. Rev.* 2001;48:139-157.

© 2016 Putra et al.; This is an Open Access article distributed under the terms of the Creative Commons Attribution License (<http://creativecommons.org/licenses/by/4.0>), which permits unrestricted use, distribution, and reproduction in any medium, provided the original work is properly cited.

Peer-review history:

The peer review history for this paper can be accessed here:
<http://sciencedomain.org/review-history/14746>